https://doi.org/10.31925/farmacia.2023.1.16 **ORIGINAL ARTICLE**

NOVEL RESVERATROL ANALOGUES WITH AROMATIC HETERO MOIETIES: DESIGNING, ONE-POT SYNTHESIS AND *IN VITRO* BIOLOGICAL EVALUATION

LAIRIKYENGBAM DEEPTI ROY [1#], JYOTSNA KUMAR [1#*], JUDY JAYS [2], GEETA KRISHNAMURTHY [1], POOJA GOUR [1], SHIVANJALI ESTHER ARLAND [1]

[1]*Department of Chemistry, M.S. Ramaiah University of Applied Sciences, Bangalore-560058, Karnataka, India*
[2]*Department of Pharmacy, M.S. Ramaiah University of Applied Sciences, Bangalore-560058, Karnataka, India*

**corresponding author: drkumarchem111@gmail.com*
[#]*Authors with equal contribution.*

Manuscript received: December 2022

Abstract

In the present work, resveratrol was used as a precursor, extracted, isolated and purified from green grapes *(Vitis vinifera*), and subjected to synthetic manipulations to acquire a series of novel resveratrol analogues. The docking results demonstrated that all three novel resveratrol analogues (ResA1, ResA2 and ResA3) can fit into the ERα (oestrogen receptor alpha) binding pockets *via* a hydrogen bond, hydrophobic and π-π interactions. *In vitro* antioxidant activity was carried out by using 1,1-diphenyl-2-picrylhydrazyl (DPPH). Results reflected that ResA2 and ResA3 exhibited high antioxidant activities than ascorbic acid used as a control. The antimicrobial activity of novel synthesized resveratrol analogues shows that *Streptococcus pneumoniae*, exhibited strong resistance to ResA3 at all concentrations. *In vitro* cytotoxic evaluation of these novel compounds on a panel of ER-positive and ER-negative human breast cancer cell lines (MCF-7, MDA-MB-231) carried out by 3-(4, 5-dimethylthiazol-2-yl)-2,5-diphenyltetrazolium bromide (MTT) assay demonstrate that ResA2 and ResA3 have potent anti-proliferative effects on both the cell lines (inhibitory concentration *i.e.*, IC50 values are 390.16 µg/mL and 327.70 µg/mL; 203.72 µg/mL and 186.58 µg/mL respectively for MCF-7 and MDA-MB-231). Synthesized resveratrol analogues had demonstrated more than 70% cell viability inhibition against human breast epithelial cell lines (MCF-10A cells), even at 500 µg/mL. This study showed that the proposed novel resveratrol analogues could be used as a plausible pharmacophore for targeting ERα protein and will be supportive for exploring the new series of resveratrol analogues as potential anticancer agents.

Rezumat

În acest studiu a fost folosit ca precursor resveratrolul, extras, izolat și purificat din struguri verzi (*Vitis vinifera*) și supus unor diferite operații pentru a obține o serie de analogi noi ai resveratrolului. Rezultatele de andocare au demonstrat că toți cei trei analogi noi ai resveratrolului (ResA1, ResA2 și ResA3) se pot lega de ERα (receptorul alfa estrogen) printr-o legătură de hidrogen, interacțiuni hidrofobe și π-π. Activitatea antioxidantă *in vitro* a fost demonstrată prin utilizarea 1,1-difenil-2-picrilhidrazil (DPPH). ResA2 și ResA3 au prezentat activități antioxidante superioare acidului ascorbic utilizat ca martor. Activitatea antimicrobiană a noilor analogi de resveratrol sintetizați a demonstrat faptul că *Streptococcus pneumoniae*, a prezentat rezistență puternică la ResA3 la toate concentrațiile. Evaluarea citotoxică *in vitro* a acestor noi compuși, determinată pe un panel de linii celulare de cancer de sân uman ER-pozitiv și ER-negativ (MCF-7, MDA-MB-231), a evidențiat că ResA2 și ResA3 au efecte anti-proliferative puternice asupra ambelor linii celulare (IC50 sunt 390,16 ug/mL și 327,70 ug/mL și respectiv 186,58 pg/mL pentru MCF-7 și MDA-MB-231). Analogii resveratrolului au demonstrat o inhibiție a viabilității celulare de peste 70% asupra liniilor celulare epiteliale ale sânului uman (celule MCF-10A), chiar și la 500 µg/mL. Acest studiu arată faptul că noii analogi ai resveratrolului propuși ar putea fi utilizați ca farmacofori pentru țintirea proteinei ERα și va sprijini explorarea noii serii de analogi ai resveratrolului ca potențiali agenți anticancerigen.

Keywords: polyphenol, drug designing, resveratrol analogue, cancer chemoprevention

Introduction

Worldwide, cancer is the second most common cause of death with almost 18.1 million new cancer cases yearly (World Health Organization). Breast cancer is considered the most diagnosed cancer in women, surpassing lung cancer. In Indian women, it accounts for 14% of cancers; every four minutes, a woman is diagnosed with breast cancer [61, 62].

Depending on the status of hormone receptors in breast cancer cells, breast cancer can be divided into four major groups: (a) hormone receptor-positive breast cancer (b) HER2+ (human epidermal growth factor receptor 2 positive) breast cancer (c) triple positive (both hormone receptor-positive and HER2+) (d) triple-negative breast cancer (absence of hormone and HER2 receptors) [7]. Literature reports that more than 70%

of breast cancers are hormone receptor-positive, particularly ER+ (oestrogen receptor positive) cancers [36, 46]. The main cause of ER-positive breast cancer (promotion of tumorigenesis and progression) is due to ERα. Consequently, controlling ERα has become a majorly challenging task for researchers [17, 38].

Despite numerous advances in technology and diagnosis, the overall cancer survival rate has not improved. After the development of various tailored methods, like chemotherapeutic treatment, targeted therapies, immunosuppression, radiation, etc., the clinical outcomes for cancer patients were shown improvement along with the attainment of resistance to the chemotherapeutic agents [13]. Thus, besides aiming for early detection, followed by proper management, the identification of drug molecules with less or negligible side effects becomes a need to fight against cancer [8]. In the case of breast cancer, the commercially available drug is tamoxifen, and another drug E-diethylstilbesterol is under clinical trials. But long-term usage of tamoxifen leads to drug resistance [45].

Epidemiological, clinical and preclinical studies have proved that secondary metabolites of plants (phyto-chemicals) play a significant role and have potent effects in controlling quite a few diseases including cancer [37, 57]. The advantageous aspects of these phytochemicals can be credited to the existence of abundant polyphenolic compounds as bioactive components, which are attributed to their rich activities such as antioxidant, anti-inflammatory, anti-fungal, antibacterial, anticancer [19, 34, 44] etc.

This invigorated the attention of scholars to the use of natural products obtained from medicinal or dietary plants as an ancillary source that can be used against diversified diseases. Hence, among researchers, there is a mushrooming interest in the usage of natural products as a probable chemo-preventive and therapeutic agent for the treatment of various diseases. Papers reported that phytochemicals like phytoestrogens are capable of modulating manifold cellular-signalling pathways, imparting negligible or minimum toxicity to normal cells [10, 60]. Subsequently, fighting cancer using phytochemicals became an attractive strategy. Literature speaks about the optimistic anticancer activity of the natural products comprising the stilbene scaffold *via* various cellular pathways. Stilbene is abundantly present in plants as a defensive bioactive component. It is produced in some plants due to the attack of pathogens or any stress [39, 41]. It is a versatile, multifaceted and copiously explored scaffold comprising two aromatic rings that are linked to each other by an ethylene bridge.

It is evident that the salient structural trait of stilbene, the presence of a double bond between two aromatic rings, impedes the proliferation of cancer cells [28]. It is noteworthy that stilbene with hetero entities displayed the highest anti-proliferative activity against most cancer cell lines [3].

Therefore, the synthesis and redesigning of stilbene analogues seek a lot of attention in medicinal chemistry. Among them, resveratrol (a natural stilbene compound) is burgeoning in prominence due to its anti-cancer properties [2, 11-12, 20]. Resveratrol, a non-flavonoid pleiotropic polyphenol belonging to the stilbene family, is a phytoalexin naturally occurring in many plants, including berries, red wine, peanuts, dark chocolates, grapes and pines. Structurally, resveratrol comprises two aromatic phenolic rings, which are connected by a double bond to give rise to 3,4′,5-trihydroxystilbene (trans- and cis-isoforms). Both cis- and trans-forms of resveratrol are found in nature, but mainly trans-resveratrol is responsible for biological activities [31] such as antioxidant [35, 50], antidiabetic [1], antifungal [51], anticancer [30, 43], anti-ageing [48]. Moreover, resveratrol is considered safe for public use since it is less cytotoxic to normal cells [5, 14, 54, 55].

Structurally, resveratrol, tamoxifen and synthetic diethylstilbesterol (DES, a synthetic form of the female hormone oestrogen under clinical trial) are quite similar. Considering the substantial potential of resveratrol as a powerful chemotherapeutic molecule and a resourceful scaffold, it has been extensively exploited by chemists, and it is often used as a lead compound to develop novel agents for various biological activities.

However, during chemotherapies, it exhibited poor bioavailability, a short half-life and less favourable pharmacokinetic variables, which encumbered its clinical trials [15, 33, 40, 47]. The poor bioavailability of resveratrol is attributable to the free hydroxyl (-OH) groups and the succeeding conjugation to sulphates and glucuronic acid which produces sulphate and glucuronide coalesce. They get amassed in urine and plasma [21, 24, 53, 59].

An extensive literature review suggested that there is a scarcity of papers reporting the anti-proliferative activity of synthesized resveratrol analogues comprising aromatic hetero entities to daunt breast tumours. In extension to our quest for a novel natural cum hetero-based anticancer agent, we selected a scaffold combination approach for the design of novel anti-breast cancer drugs. On the basis of the literature, we designed novel resveratrol analogues comprising aromatic hetero entities (Figure 1) by doing synthetic manipulation on a resveratrol scaffold to improve its bioavailability, provide superior pharmacokinetics and enhance its biological activities.

However, the synthesis of drug molecules, their characterization and the study of their biological activities involve several chemical reactions and tiresome biological and cell-line experiments, which devour a lot of time in due course. As a result, the current study began with the designing of novel drug

molecules containing resveratrol and aromatic hetero moieties. After a virtual screening of the designed resveratrol analogues with the target protein, the best resveratrol analogues showing better binding ability were subjected to a one-pot synthetic scheme by using natural resveratrol extracted and isolated from the green grape (*Vitis vinifera*) peels. Structures of the synthesized molecules were elucidated by NMR, FTIR and mass spectroscopic methods. For all three synthesized novel resveratrol analogues, *in silico* pharmacokinetics, toxicity and *in vitro* biological activities were carried out, such as antioxidant (using DPPH), antimicrobial (fungal, Gram-positive and Gram-negative bacterial strains) and anticancer activity (MCF-7, MDA-MB-231, MCF-10A cell lines using MTT assay).

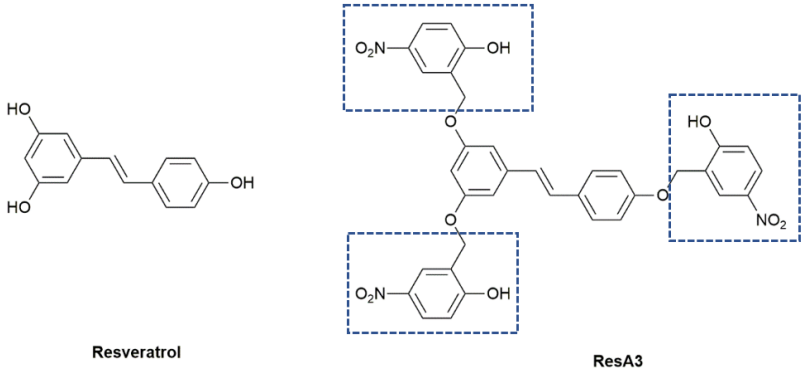

Figure 1.
Chemical structures of Resveratrol and its hybrid. The aromatic hetero entity is depicted with the blue (-----) lines

Materials and Methods

Molecular modelling for the identification of hit molecules

3D structure of oestrogen receptor alpha (ERα; PDB ID 2iok) was retrieved from Protein Data Bank [9] (Figure 2).

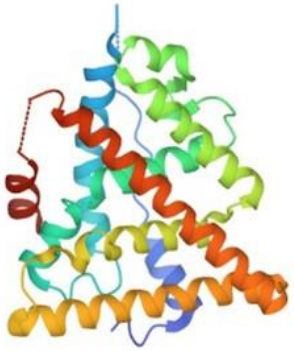

Figure 2.
3D structure of ERα (PDB ID 2iok)

Ligand structures *i.e.*, resveratrol (parent compound), tamoxifen (control) and newly designed resveratrol analogues with aromatic hetero moieties (Figure 3) were prepared using ChemDraw Ultra 12.0 [23]. OpenBabel software [49] was used for the conversion of files. The protein structure was modified – deleted water molecules, side chains and heteroatoms; added missing residues and Kollman charges using Molecular Graphics Laboratory (MGL) Tools (AutoDock 4.0). AutoDock 4.0 and AutoGrid 4.0 were used to generate a grid box with 0.5 Å spacing and by choosing the identified active sites of the protein thereby creating grid log files. In continuation, molecular docking was carried out using the same software using generic algorithm (GA) parameter and Lamarckian GA as output file thereby obtaining a docking log file which contains detailed information on the ligand-protein interaction. Graphic manipulations and visualization were done by MGL tools and Protein-Ligand Interaction Profiler (PLIP) [27].

Materials

All chemical reagents (AR grade; 98% purity) were purchased from Sigma Aldrich or TCI Chemicals: 1,1-diphenyl-2-picrylhydrazyl (DPPH), Dulbecco's Modified Eagle Medium (DMEM) high glucose media (cell culture medium), foetal bovine serum (FBS), 3-(4,5-Dimethylthiazol-2-yl)-2,5-Diphenyltetrazolium Bromide (MTT) reagent, Dimethyl Sulfoxide (DMSO) and Mueller Hinton agar from HiMedia, Mumbai, were used without further purification. Bacterial strains: Gram-positive - *Staphylococcus aureus* (MTCC 96), *Bacillus subtilis* (MTCC 441), *Streptococcus pneumoniae* (MTCC 655); Gram-negative - *Escherichia coli* (MTCC 443), *Klebsiella pneumoniae* (MTCC 7162), *Pseudomonas aeruginosa* (MTCC 424) and fungal strains: *Candida albicans* (MTCC 227) and *Trichophyton mentagrophytes* (MTCC 7687) were obtained from MTCC, IMTECH, Chandigarh, India. Cell lines MCF-7, MDA-MB-231 and MCF-10A were obtained from NCCS, Pune, India.

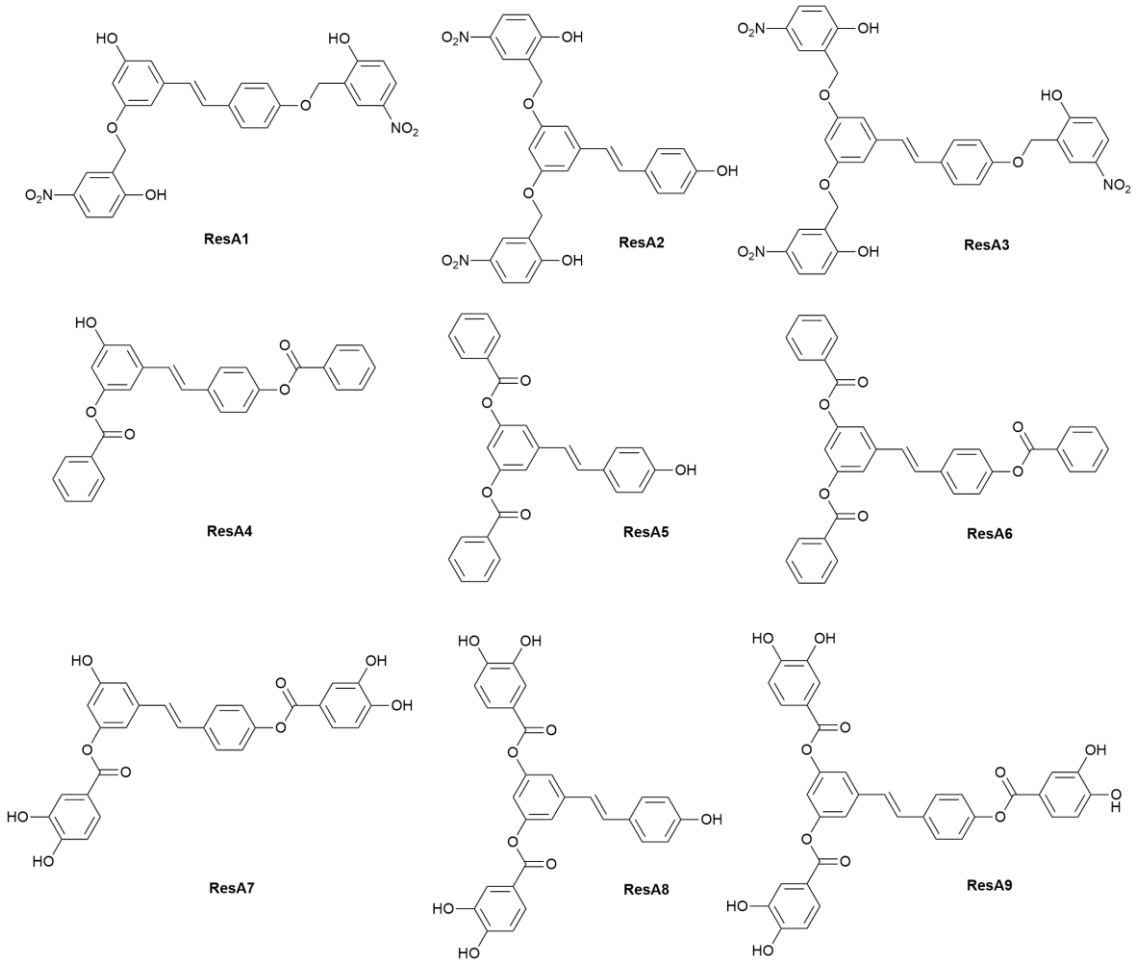

Figure 3.
Newly designed structures of resveratrol analogues bearing aromatic hetero entities (ResA1-A9)

Methods

Chemical reactions were monitored by thin-layer chromatography (TLC) on Merck TLC plates and were analysed using a 254/365 nm UV (ultraviolet) lamp. CombiFlash RF 200 (Teledyne ISCO) was used for chromatography. ThermoFisher Scientific's NicoletTM iS20 Fourier transform infrared (FTIR) Spectrometer was used to capture attenuated total reflection infrared (ATR-IR) spectra. ^{1}H and ^{13}C Nuclear Magnetic Resonance (NMR) were recorded on a 400 MHz NMR spectrometer (Bruker) using tetramethylsilane (TMS) as an internal reference and chemical shifts were reported in ppm (parts per million, δ units). Splitting patterns are designed as s, singlet; d, doublet; dd, doublet of doublet; b, broad; m, multiplet. Liquid Chromatography-Mass Spectroscopy (LC-MS) data were recorded on an LC-40, high-performance liquid chromatography (HPLC) System (Shimadzu). Bacteriological incubator Sandhya clean air Equipment, Model.No:SA01 was used for *in vitro* biological activities.

Extraction, isolation and purification of resveratrol from grape peels

200 g of ground and sieved (150 mm) dried grape skin powder was soaked in a 2500 mL ethanol/water (80:20) solution for 1 hour in a 5000 mL three-neck round bottom flask and maintained at 78°C for 3 hours with gentle stirring. The extract was filtered through a Whatman No 1 filter paper. The whole process was repeated twice. The total filtrate collected was concentrated up to 10% using a Rota-evaporator. The concentrated extracts were filtered through the Whatman membrane filters. To estimate the content of resveratrol present in the crude extract, injected the extract into the HPLC without further processing, along with standard resveratrol. Further purification was done by flash chromatography using 60 - 120 mesh size silica gel and hexane and ethyl acetate (50:50) as solvents. Structure elucidation of the isolated resveratrol (off-white solid; 89% yield) was executed by NMR, FTIR and LCMS spectral analysis.

5-[(E)-2-(4-Hydroxyphenyl)ethen-1-yl]benzene-1,3-diol (Resveratrol obtained from green grapes)

^{1}H NMR, 400 MHz, DMSO-d6 (ppm): 9.53 (s, 1H), 9.17 (s, 2H), 7.39 (d, 2H, J = 8.4 Hz), 6.94 (d, 1H, J = 16.4Hz), 6.82 (d, 1H, J = 16.4 Hz), 6.73 (d, 2H, J = 8.4 Hz), 6.37 (d, 2H, J = 2 Hz), 6.11 (t, 1H, J = 3.6 Hz); ^{13}C NMR, 400 MHz, DMSO-d6 (ppm): 158.534, 157.236, 139.297, 128.089, 125.668, 127.891, 115.545, 104.321, 101.787; IR ATR (cm^{-1}): 3456 (-OH), 1601

(C=C); LC-MS (m/z, ESI+ve, $C_{14}H_{12}O_3$): Calculated mass was 228.24, observed mass found was 229.13 $(M+H)^+$.

General Method for the Synthesis of Resveratrol Analogues (ResA1, ResA2 and ResA3)

The condensation reaction was carried out by adding dimethyl formamide (DMF; 750 mL) in a 1000 mL three-neck round bottom flask fitted in a reflux condenser with an oil bath, adding resveratrol (10 g) with continuous stirring, and adding anhydrous potassium carbonate (30 g). The reaction mixture was stirred for 45 minutes. After that, 2-bromomethyl-4-nitrophenol (35.5 g) and potassium iodide (0.73 g) were added to the reaction mixture. The reaction mass was heated at a reflux temperature (120°C) with continuous stirring until the completion of the reaction. The reaction progress was monitored throughout by TLC and LCMS with the solvent system (EtOAc and methanol). The mixture was allowed to cool and extracted with dichloromethane. The organic phase was dried over magnesium sulphate and evaporated to obtain a solid residue containing a mixture of ResA1, ResA2 and ResA3 (crude product).

The crude product yielded 30 g. It was purified by column chromatography using 60 - 120 mesh size silica gel and a mixture of ethyl acetate and methanol as eluents to separate the desired products. When 100% ethyl acetate was taken as eluent, a light brown solid (ResA3) was eluted first with a yield of 35%. Next, an eluent of 90:10 ethyl acetate and methanol mixture was used to elute a light-yellow solid (ResA1) bearing a 20% yield. In the same chromatographic system (90:10 ethyl acetate and methanol mixture), a dark yellow solid (ResA2) was eluted last with a 22% yield.

(E)-2-((4-(3-hydroxy-5-((2-hydroxy-5-nitrobenzyl)-oxy)styryl)phenoxy)methyl)-4-nitrophenol (ResA1)

^{1}H NMR, 400 MHz, DMSO-d6 (ppm): 9.693 (2H, b); 9.155 (1H, s); 7.913 (2H, m); 7.566 (2H, dd, J = 2.8 Hz, 2.8 Hz); 7.380 (2H, d, J = 20.4 Hz); 7.222 (1H, d, J = 30.4 Hz); 7.012 (1H, d, J = 10 Hz); 6.106 (7H, m); 5.080 (4H, s); ^{13}C NMR, 400MHz, DMSO-d6 (ppm): 162.061, 160.439, 160.249, 159.968, 159.666, 157.105, 140.599, 140.088, 137.786, 129.907, 129.624, 127.991, 127.764, 127.540, 127.399, 126.216, 124.295, 124.090, 121.991, 121.655, 117.727, 17.269, 115.542, 115.406, 104.026, 102.447, 100.830, 59.362; IR ATR (cm^{-1}): 3456 (-OH), 1517 and 1343 (-NO_2), 1645 (C=C); LC-MS (m/z, ESI+ve, $C_{28}H_{22}N_2O_9$): The calculated mass was 530.48, and the found mass was 530.95 $(M+H)^+$

(E)-2,2'-(((5-(4-hydroxystyryl)-1,3-phenylene)bis-(oxy))bis(methylene))bis(4-nitrophenol) (ResA2)

^{1}H NMR, 400 MHz, DMSO-d6 (ppm): 9.394 (3H, b); 8.092 (2H, m); 7.913 (2H, m); 7.377 (2H, d, J = 26.8 Hz); 7.010 (1H, d, J = 13.6 Hz); 6.989 (1H, d, J = 8 Hz); 6.112 (7H, m); 5.080 (4H, s); ^{13}C NMR, 400 MHz, DMSO-d6 (ppm): 161.665, 161.408, 160.386, 160.299, 155.083, 140.486, 138.108, 130.227, 129.204, 128.496, 128.036, 127.996, 127.363, 127.042, 123.994, 123.109, 121.286, 117.387-117.843, 115.389, 115.464, 102.918, 102.283, 99.689, 59.686; IR ATR (cm^{-1}): 3248 (-OH), 1586 and 1328 (-NO_2), 1605, 1614, 1633 (C=C); LC-MS (m/z, ESI+ve, $C_{28}H_{22}N_2O_9$): The calculated mass was 530.48 and the measured mass was 531.45 $(M+H)^+$

(E)-2,2'-(((5-(4-((2-hydroxy-5-nitrobenzyl)oxy)-styryl)-1,3 phenylene)bis(oxy))bis(methylene))bis(4-nitrophenol) (ResA3)

^{1}H NMR, 400 MHz, DMSO-d6 (ppm): 9.456 (3H, b); 7.913 (6H, m); 7.587 (2H, d, J = 10.8 Hz); 7.068 (1H, d, J = 18.4 Hz); 7.012 (1H, d, J = 10 Hz); 6.106 (7H, m); 5.475 (6H, s); ^{13}C NMR, 400MHz, DMSO-d6 (ppm): 161.661, 161.362, 160.509, 160.241, 160.068, 159.666, 141.105, 140.999, 139.888, 137.786, 129.924, 129.235, 127.991, 127.764, 127.240, 123.595, 123.390, 123.091, 121.655, 117.269-117.542, 114.802, 114.487, 104.026, 102.447, 100.800, 58.562; IR ATR (cm^{-1}): 3455 (-OH), 1543 and 1317 (-NO_2), 1595, 1645, 1630 (C=C); LC-MS (m/z, ESI+ve, $C_{35}H_{27}N_3O_{12}$): Calculated mass was 681.6 and the measured mass was 682.31 $(M+H)^+$

In silico ADMET prediction

Physicochemical properties, medicinal chemistry and ADMET (Absorption, Distribution, Metabolism, Excretion and Toxicity) properties of the parent compound (resveratrol), the standard drug (tamoxifen) and the synthesized compounds (ResA1, ResA2 and ResA3) were evaluated by using ADMETLab 2.0 [56].

Biological assays

DPPH free-radical-scavenging activity

The free-radical-scavenging activity of ResA1, ResA2 and ResA3 on the DPPH radical was estimated as per the standard procedure [52]. 50 µL of a methanolic solution of the synthesized novel derivatives was added to a 6 x 10^{-5} M methanolic solution of DPPH. Different concentrations (0 µg/mL, 9.37 µg/mL, 18.7 µg/mL, 37.5 µg/mL, 75 µg/mL and 150 µg/mL) of the synthesized molecules were taken to measure the absorbance. A spectrophotometer set at 515 nm was used to record the absorbance for 16 min at room temperature. The pure chemical (control) was evaluated in methanolic solutions at a concentration of 1 µg/mL. The scavenging effect was plotted against time, and the samples' (ResA1, ResA2 and ResA3) percentage of DPPH radical scavenging ability was derived from the absorbance value using the formula [58]:

$$\% \text{ Radical scavenging activity of DPPH} = [(A_0 - A_1)/A_0) \times 100,$$

where A_0 is the absorbance of the control, and A_1 is the absorbance of the test drug. The percentage of inhibition was then plotted against concentration, and the IC50 was calculated from the graph. The experiment was performed in triplicate.

Evaluation of the Zone of Inhibition (ZOI) of ResA1, ResA2 and ResA3 and the control group (azithromycin) against Gram-positive and Gram-negative bacteria

Agar well diffusion techniques (Kirby-Bauer process) were used to measure the antibacterial activity [16, 18]. Each sterile Petri plate was filled with approximately 25 mL of molten Mueller Hinton agar. Afterwards, 100 µL of the aforementioned bacteria (cultured for 18 h with the optical density set to 0.6) were put onto a plate and converted into a culture lawn using a sterile L-rod spreader. Once all microorganisms had set for five minutes, a 6 mm well was made on the agar with a sterile cork borer. ResA1, ResA2 and ResA3 test samples were dispensed into wells at various concentrations of 50 µg/well, 100 µg/well, 150 µg/well and 200 µg/well. As a positive control, azithromycin (30 µg/well) was used. In a bacteriological incubator, all prepared plates were incubated for 24 h at 37°C. Using the antibiotic zone scale, the diameter of the ZOI was measured to estimate the anti-microbial activity. There were three duplicates of the experiment.

Evaluation of the Zone of Inhibition of ResA1, ResA2, ResA3 and the Control Group (clotrimazole) against Fungal Strains

The antifungal activity was also assessed using the Agar Well Diffusion Method [26]. The test samples (ResA1, ResA2 and ResA3) were loaded into wells with different concentrations of 50 µg/well, 100 µg/well, 150 µg/well and 200 µg/well. The clotrimazole (30 µg/well) was used as a positive control. The antifungal activity was determined by measuring the diameter of the zone of inhibition using the antibiotic zone scale. The experiment was performed in triplicate.

MTT assay to assess the viability of MCF-7, MDA-MB-231 and MCF-10A cells after exposure to ResA1, ResA2, ResA3 and the standard drug (tamoxifen)

200 µL cell suspension was seeded in a 96-well plate at the required cell density (2 x 10^4 cells *per* well), without the test agent and added appropriate concentrations of the test agents (ResA1, ResA2 and ResA3) in a dose-dependent manner (31.25, 62.5, 125, 250 and 500 µg/mL) respectively. The plate was incubated for 24 h at 37°C in a 5% CO_2 atmosphere. After the incubation period, plate was taken out of the incubator, removed spent media, and added the MTT reagent to a final concentration of 0.5 mg/mL of total volume. The plate was allowed to return to the incubator and incubated for 3 h, removed the MTT reagent and then added 100 µL of solubilization solution (DMSO). Medium control (medium without cells), negative control (medium with cells but without the experimental compound) and positive control (medium with cells and 25 µM of tamoxifen) were used as assay controls. The absorbance was read on a spectrophotometer at 570 nm and 630 nm using a reference wavelength [29]. Each experiment was performed in triplicate. Concentration–cell viability curves were fitted and their IC50 values were determined by using a linear regression equation *i.e.*, Y = Mx + C where Y = 50 and M and C values were derived from the cell viability graph.

Results and Discussion

Designing and screening of hit molecules

Docking scores were obtained after AutoDock docking calculations (Table I). Out of the newly designed molecules, the docking score of ResA2 is -9.51 kcal/mol, which is higher than that of resveratrol (-5.11 kcal/mol) and tamoxifen (-4.98 kcal/mol); followed by ResA3 (-8.48 kcal/mol) and ResA1 (-7.50 kcal/mol). The remaining designed molecules (*i.e.*, ResA4 to ResA9) have docking scores in the range of 3 - 7 kcal/mol. Hence ResA1, ResA2 and ResA3 are identified as hit molecules and further synthesized to assess their *in vitro* biological activities.

Table I

Docking scores of newly designed resveratrol analogues with aromatic hetero moiety

Code no	Binding score (kcal/mol)	Code no	Binding score (kcal/mol)	Code no	Binding score (kcal/mol)
ResA1	-7.50	ResA4	-5.53	ResA7	-6.65
ResA2	-9.51	ResA5	-3.74	ResA8	-7.47
ResA3	-8.48	ResA6	-3.50	ResA9	-6.93

PLIP was used to visualize the interaction of ERα and ResA1, ResA2 and ResA3, respectively (Figure 4). ResA1 does not show any hydrogen bond interactions with ERα. The other two resveratrol analogues *i.e.* ResA2 and ResA3 as well as parent compound and control were showing hydrogen bond interaction with several amino acids of ERα such as resveratrol with 327A Leu (2.57 Å, H-A; 3.45 Å, D-A), tamoxifen with 323A Glu (1.93 Å, H-A; 2.61 Å, D-A), ResA2 with 323A Glu (2.03 Å, H-A; 2.53 Å, D-A), 394A Arg (3.75 Å, H-A; 4.07 Å, D-A) and 449A Lys (3.28 Å, H-A; 4.04 Å, D-A), ResA3 with 393A Trp (2.75 Å, H-A; 3.77 Å, D-A) and 449A Lys (2.30 Å, H-A; 3.32 Å, D-A).

Chemistry

Extraction, isolation and purification of resveratrol from dried grape peel powder were done as shown in Figure 5. Synthesis of novel resveratrol derivatives (ResA1, ResA2 and ResA3) was done by the condensation reaction (Figure 6).

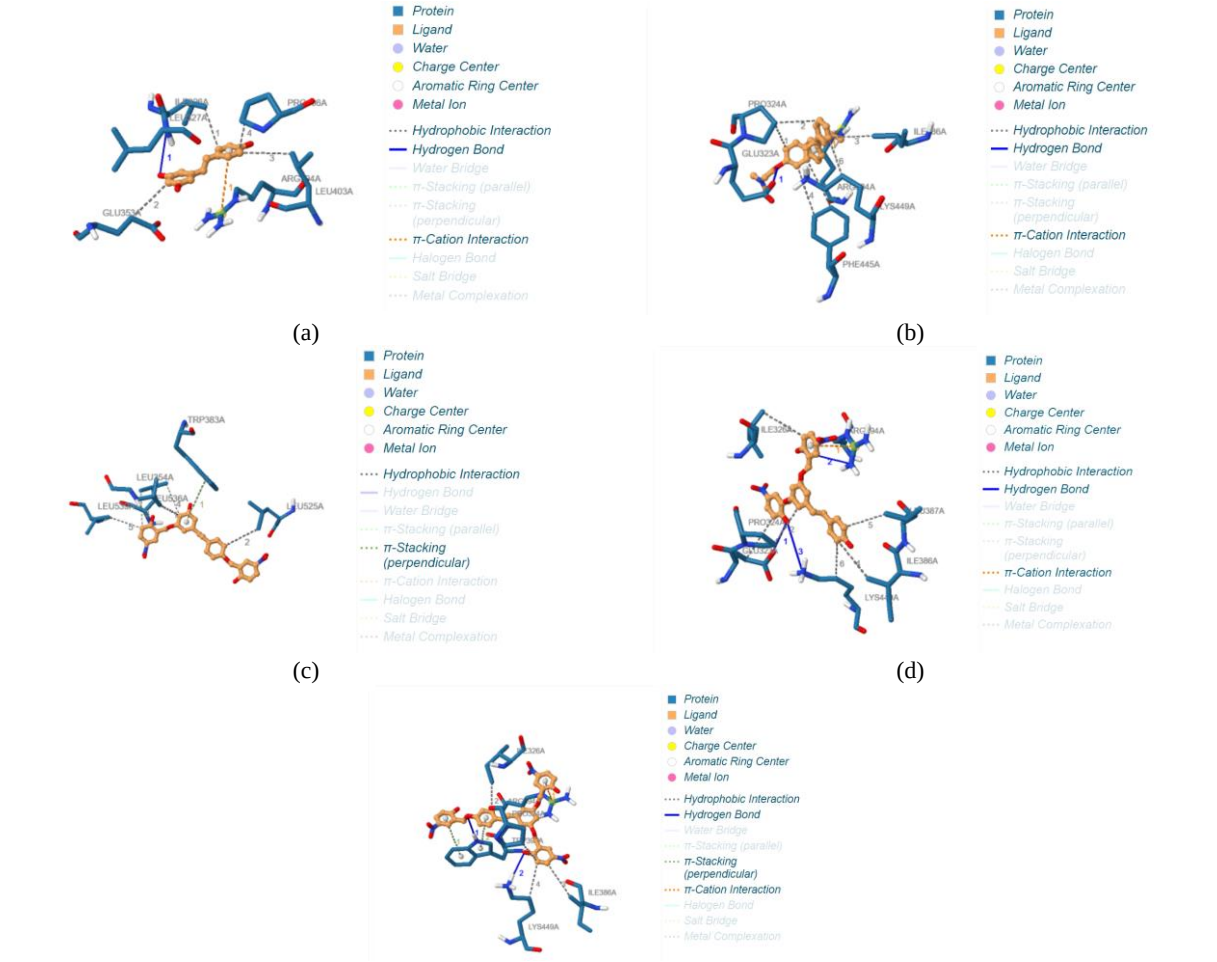

Figure 4.

View of Estrogen receptor alpha binding pockets. Panels show the posing of (a) Resveratrol (b) Tamoxifen (c) ResA1 (d) ResA2 and (e)ResA3

In silico ADMET prediction

The results of ADMETLab 2.0 are shown in Table II. All three synthesized molecules (ResA1, ResA2 and ResA3) violate the Lipinski rule of 5 and the Pfizer rule. An alternative approach to the human intestinal epithelium, the Caco-2 (human colon adeno-carcinoma) cell line, is commonly used to estimate drug permeability. Out of the three molecules, only ResA1 is Caco-2 permeable. Papp for MDCK (Madin-Darby Canine Kidney) is considered a gold standard to assess the uptake efficiency of drugs into the human body. All synthesized analogues (ResA1, ResA2 and ResA3) showed medium MDCK permeability.

Undoubtedly, oral bioavailability is an important pharmacokinetic property to check how efficiently the drug is delivered to the systemic circulation. All the molecules are F30%+ (human oral bioavailability 30%).

The Volume of Distribution (VD) represents the obvious volume into which the drug molecule is distributed to offer the same concentration as it currently is in blood plasma. ResA1, ResA2 and ResA3 exhibited optimum VD since their values are in the optimal range of 0.04 - 20 L/kg. The positive blood-brain barrier (BBB+) value of all three resveratrol analogues indicates that they can act on the Central Nervous System (CNS) as they can cross the blood-brain barrier to reach the target. The fraction unbound in plasma (Fu) specifies the drug's efficiency at binding to proteins in human membranes. Lower Fu values for ResA1 and ResA3 indicated that their distribution in the human body was better than ResA2.

Checking the potential of a drug molecule to hinder a particular cytochrome P450 enzyme (CYP isoforms – CYP 1A2 / 2C19 / 2C9 / 2D6 / 3A4) is certainly significant as this interaction may also affect the plasma levels and possibly lead to toxicity. All the synthesized resveratrol analogues were found to be inhibitors of cytochrome 450 enzymes. One important pharmacokinetic property of a drug is drug clearance and half-life. ResA1, ResA2 and ResA3 displayed moderate clearance rates, but only ResA1 and ResA2 showed good half-life (medium). ResA3 had a short half-life (poor half-life).

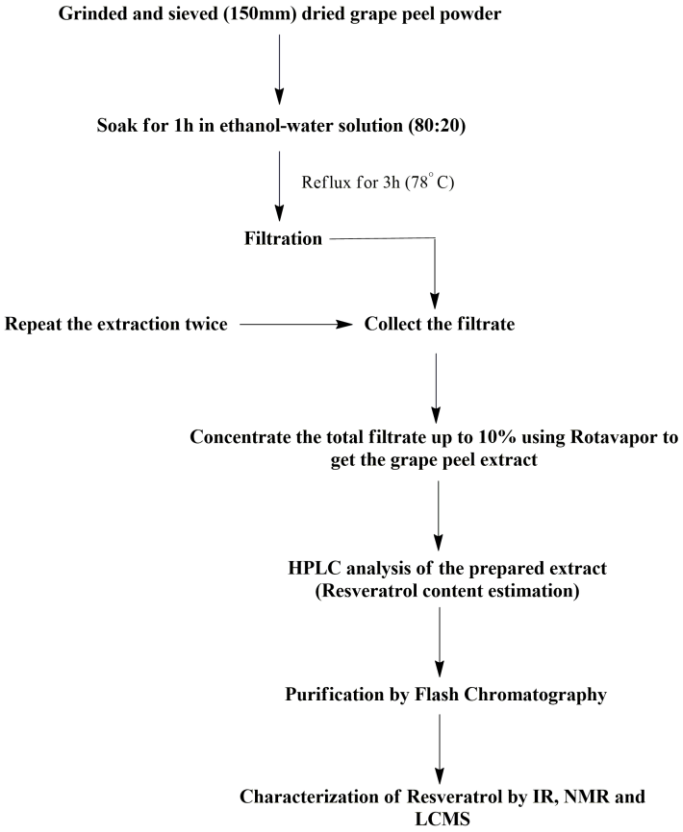

Figure 5.
Extraction, isolation and purification of Resveratrol from grape peel

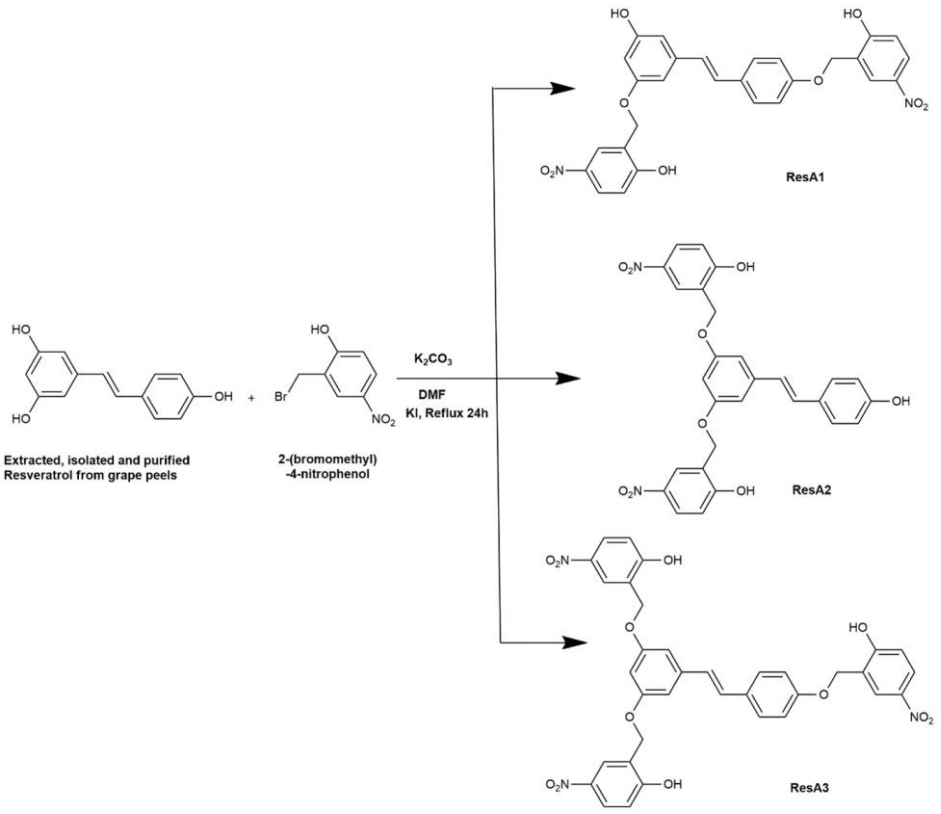

Figure 6.
Schematic plan for the synthesis of novel resveratrol analogues with the best docking scores; 3, 4′di-substitution (ResA1), 3,5 di-substitution (ResA2) and 3, 5, 4′ tri-substitution (ResA3)

Table II

Physicochemical, drug-likeness and ADMET data of ResA1, ResA2 and ResA3

Physicochemical property	**Optimal condition**	**ResA1**	**ResA2**	**ResA3**
Molecular weight	*100 - 600 g/mol*	530.13	530.13	681.16
nHA (Number of hydrogen bond acceptor)	*0 - 12*	11	11	15
nHD (Number of hydrogen bond donor)	*0 - 7*	3	3	3
nRot (Number of rotable bond)	*0 - 11*	10	10	14
nRing (Number of rings)	*0 - 6*	4	4	5
TPSA (Topological Polar Surface Area)	*0 - 140*	165.4	165.43	217.8
logS (Log of the aqueous solubility)	*-4 - 0.5 log mol /L*	-4.32	-4.45	-4.383
logP (Log of the octanol/water partition co-efficient)	*0-3*	4.543	4.946	5.631
logD (Log P at physiological pH 7.4)	*1 - 3*	3.977	4.322	4.262
Medicinal chemistry	**Rules**	**ResA1**	**ResA2**	**ResA3**
Lipinski rule	*MW ≤ 500; logP ≤ 5; nHA ≤ 10; nHD ≤ 5*	Rejected	Rejected	Rejected
Pfizer Rule	*MW ≤ 400; logP ≤ 4*	Rejected	Rejected	Rejected
Absorption	**Optimal condition**	**ResA1**	**ResA2**	**ResA3**
Caco-2 Permeability	*Higher than -5.15 log unit*	-5.133	-5.254	-5.326
MDCK (Madin−Darby Canine Kidney) Permeability (in Papp)	*Low permeability: < 2 × 10^{-6} cm/s; Medium permeability: 2 - 20 × 10^{-6} cm/s; High passive permeability: > 20 × 10^{-6} cm/s*	6.3 x 10^{-6} (medium)	8.7 x 10^{-6} (medium)	23.4 x 10^{-6} (high)
$F_{20\%}$ (20% bioavailability)	*$F_{20\%}$+ (bioavailability 0 to 1); $F_{20\%}$- (bioavailability ≤ -1)*	0.0 ($F_{20\%}$+)	0.0 ($F_{20\%}$+)	0.0 ($F_{20\%}$+)
Distribution	**Optimal condition**	**ResA1**	**ResA2**	**ResA3**
VD (Volume Distribution)	0.04 - 20 L/kg	0.31	0.372	0.152
BBB (Blood-Brain Barrier) penetration	*BBB + (logBB > -1) BBB- (logBB ≤ -1) Empirical decision: 0 - 0.3: excellent; 0.3 - 0.7: medium; 0.7 - 1.0: poor*	0.366 (BBB+; medium)	0.379 (BBB+; medium)	0.504 (BBB+; medium)
Fu (Fraction unbound in plasms)	*> 20%: High Fu; 5 - 20%: Medium Fu; < 5%: Low Fu*	0.463% (low)	0.501% (medium)	0.369% (low)
Metabolism	**Optimal condition**	**ResA1**	**ResA2**	**ResA3**
CYP1A2 inhibitor	*Category 0: Non-inhibitor (no); Category 1: inhibitor (yes)*	yes	yes	yes
CYP2C19 inhibitor		yes	yes	yes
CYP2C9 inhibitor		yes	yes	yes
CYP2D6 inhibitor		yes	yes	yes
CYP3A4 inhibitor		yes	yes	yes
Excretion	**Optimal condition**	**ResA1**	**ResA2**	**ResA3**
CL (Clearance)	*High: > 15 mL/min/kg; moderate: 5 - 15 mL/min/kg; low: < 5 mL/min/kg*	9.732 (Moderate)	10.727 (Moderate)	8.067 (Moderate)
$T_{½}$ (Half-life)	*Empirical decision: 0 - 0.3: short; 0.3 - 0.7: medium; 0.7 - 1.0: poor*	0.42 (medium)	0.624 (medium)	0.19 (short)
Toxicity	**Optimal condition**	**ResA1**	**ResA2**	**ResA3**
hERG (Human ether-a-go-go related gene) Blockers	*Range: 0 to 1 Empirical decision: 0 - 0.3: less blockade; 0.3 - 0.7: medium blockade; 0.7 - 1.0: high blockade*	0.222 (Less blockade)	0.24 (Less blockade)	0.119 (Less blockade)
H-HT (Human Hepatotoxicity)	*Range: 0 to 1 Empirical decision: 0 - 0.3: less toxic; 0.3 - 0.7: toxic; 0.7 - 1.0: very toxic*	0.1 (Less toxic)	0.51 (Toxic)	0.073 (Less toxic)
AMES toxicity	*Range: 0 - 1 Empirical decision: 0 - 0.3: less toxic; 0.3 - 0.7: toxic; 0.7 - 1.0: very toxic*	0.97 (Very toxic)	0.976 (Very toxic)	0.963 (Very toxic)

The toxicity profile of novel synthesized resveratrol analogues revealed that ResA1 and ResA2 are more hERG+ (human ether-a-go-go-related gene) than ResA3, *i.e.*, ResA1 and ResA2 can block hERG, leading

to fainting, palpitations, or even sudden death. Further human hepatotoxicity results (drug-induced liver injury) explicate that ResA1 and ResA3 are less toxic in comparison to ResA2 in the human liver. Ames's test was positive for all three resveratrol analogues. This elucidates that all three are mutagenic by nature.

Antioxidant activity of ResA1, ResA2 and ResA3

DPPH is the most used free radical in antioxidant activity evaluation, and it can accept hydrogens. It is considered a stable free radical because of the delocalization of the spare electron over the molecule (Figure 7). The violet colour of DPPH in ethanol solution (absorbance at 520 nm) is due to this delocalization. When this DPPH solution is mixed with a hydrogen atom donor molecule, DPPH is reduced, and its violet colour disappears. The primary reaction is Z* + AH = ZH + A*, where Z* is the DPPH radical, AH is the donor molecule, ZH is the reduced form, and A* is the free radical produced [22].

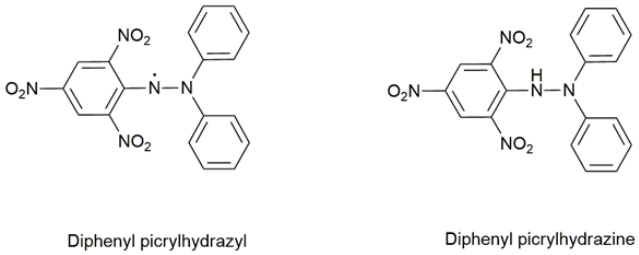

Figure 7.
Delocalisation of the spare electron of DPPH - free radical (unstable form) and non-radical (stable form

The colour reduction of DPPH and DPPH free radical scavenging ability of ResA1, ResA2 and ResA3 are shown in Figures 8 and 9. All three compounds showed DPPH radical scavenging activity in a dose-dependent manner. ResA3 showed the highest inhibition ability of DPPH free radical oxidation, followed by ResA2; ResA1 showed the lowest inhibition ability. Based on the IC50 values, the antioxidant activities of ResA3 (IC50 = 26.82 µg/mL) and ResA2 (39.54 µg/mL) were stronger than ascorbic acid (43.2 µg/mL) used as control.

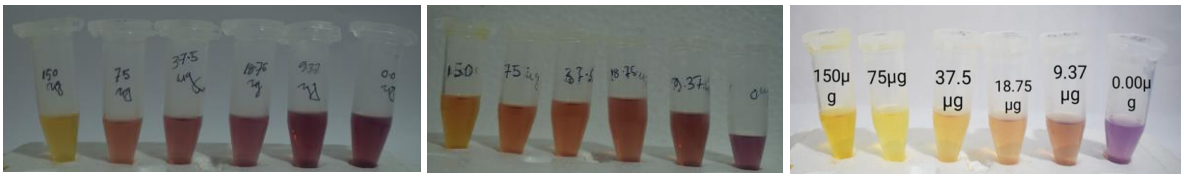

Figure 8.
Colour reduction of DPPH by ResA1, ResA2 and ResA3 (left to right)

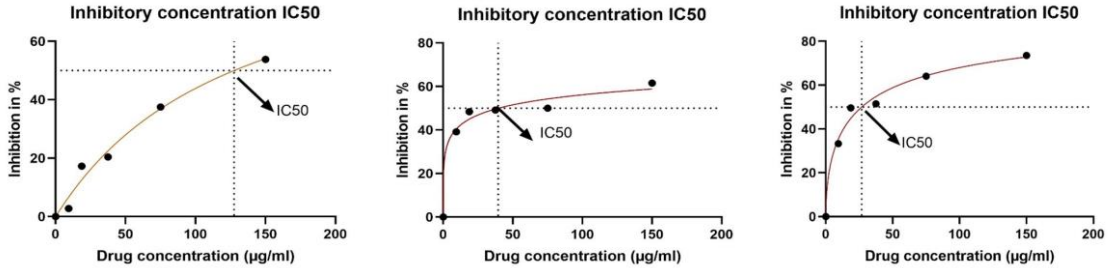

Figure 9.
Inhibition % vs drug concentration of ResA1, ResA2 and ResA3 (IC50 values are 127.6 µg/mL, 39.54 µg/mL and 26.82 µg/mL respectively from left to right)

Antimicrobial activity of ResA1, ResA2 and ResA3

To develop a more efficacious drug molecule, evaluation of antimicrobial activity, a prerequisite constraint is required [25, 32, 42]. The agar diffusion method developed by Bauer and Kirby is a widely used assay for the determination of antimicrobial activity. The effect of the drug is correlated with the inhibition zone produced around the well. The greater the ZOI value, the better the anti-microbial activity [6]. Results showed that the ZOI values of novel drug molecules (ResA1, ResA2 and ResA3) increase in a dose-dependent manner (50 to 200 µg/mL) against both bacterial and fungal strains. Interestingly, even at the highest concentration (200 µg/mL), ResA2 and

ResA3 showed no antibacterial activity against *B. subtilis*, which is a non-pathogenic bacterium. ResA3 was not able to induce *S. pneumoniae* cell death at any concentrations. Overall, all the derivatives exhibited strong antimicrobial activity but were weaker than the standard drugs (Table III). Since ResA2 and ResA3 do not affect the non-pathogenic bacteria *B. subtilis*, we can predict that ResA2 and ResA3 are better antimicrobial agents than ResA1. And ResA2 is the best antimicrobial agent among the three derivatives since it killed all the tested microbial strains.

Table III

Zone of inhibition (ZOI) of synthesised compounds (ResA1, ResA2 and ResA3) against microbial strains

	ZOI (mm)				
	ResA1	**ResA2**	**ResA3**	***Azithromycin**	***Clotrimazole**
Gram-positive					
S. aureus (MTCC 96)	15	9	16	20	-
B. subtilis (MTCC 441)	8	na	na	14	-
S. pneumoniae (MTCC 655)	7	13	na	17	-
Gram-negative					
E. coli (MTCC 443)	13	13	14	18	-
K. pneumoniae (MTCC 7162)	13	9	9	25	-
P. aeruginosa (MTCC 424)	9	14	12	16	-
Fungi					
C. albicans (MTCC 227)	10	9	9	-	20
T. mentagrophytes (MTCC 7687)	12	7	9	-	23

Note: ZOI is observed at 200 µg/mL; *standard drugs used (30µg/well); na indicates not affected

Cytotoxicity of ResA1, ResA2 and ResA3 against MCF-7, MDA-MB-231 and MCF-10A cell lines

MTT assay, to determine cell proliferation and cytotoxicity is based on the reduction of MTT (yellow-coloured water-soluble tetrazolium salt) to form insoluble, blue-coloured formazan crystals by mitochondrial enzymes, which upon dissolution into an appropriate solvent display a purple colour, the intensity of which is proportional to the number of viable cells and can be measured spectrophotometrically at 570 nm [4, 29]. On MCF-10A cell lines, all three compounds (ResA1, ResA2 and ResA3) have almost no cytotoxic effect, even at the highest concentration (500 µg/mL). Except for ResA1, ResA2 and ResA3 were cytotoxic to MCF-7 (ER-positive) as well as MDA-MB-231 (ER-negative) cell lines. IC50 values of ResA2 and ResA3 against MCF-7 cells were 390.16 µg/mL and 327.70 µg/mL respectively whereas, IC50 values were 203.72 µg/mL and 186.58 µg/mL against MDA-MB-231 cells. Thus, ResA2 and ResA3 have potent cytotoxic effects against MCF-7 and MDA-MB-231 cells, but they are weak cytotoxic compared to resveratrol (IC50 = 29.89 µg/mL) [43]. No IC50 value was obtained for ResA1 against both MCF-7 and MDA-MB-231 cells. Compared to the standard drug (tamoxifen), cell viability of both the breast cancer cell lines on exposure to ResA2 and ResA3 decreased in a dose-dependent manner (Figure 10 and Figure 11) and cell viability was reduced to 40% at the highest concentration (500 µg/mL).

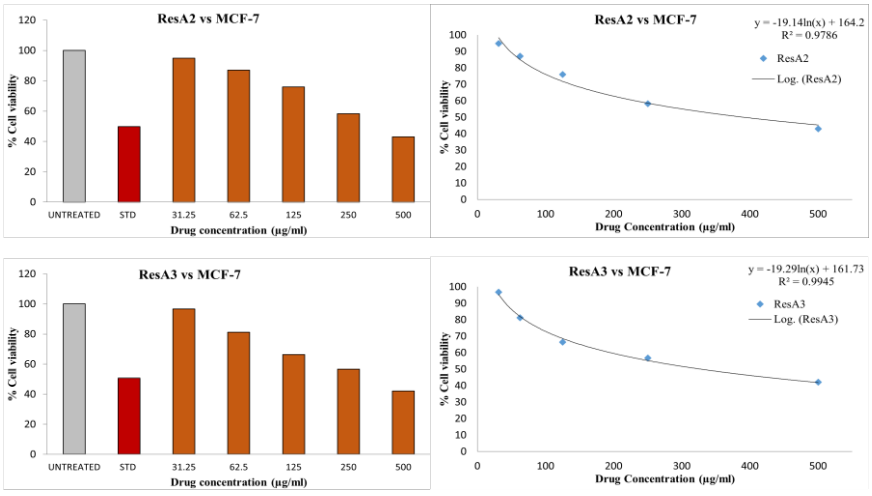

Figure 10.

% Cell viability vs drug concentration graphs in a dose-dependent manner and IC50 graphs of ResA2 (IC50 = 390.16 µg/mL) and ResA3 (327.70 µg/mL); tamoxifen as a standard drug against MCF-7 cells. The data shown are the means of three replicates and are expressed as percentages

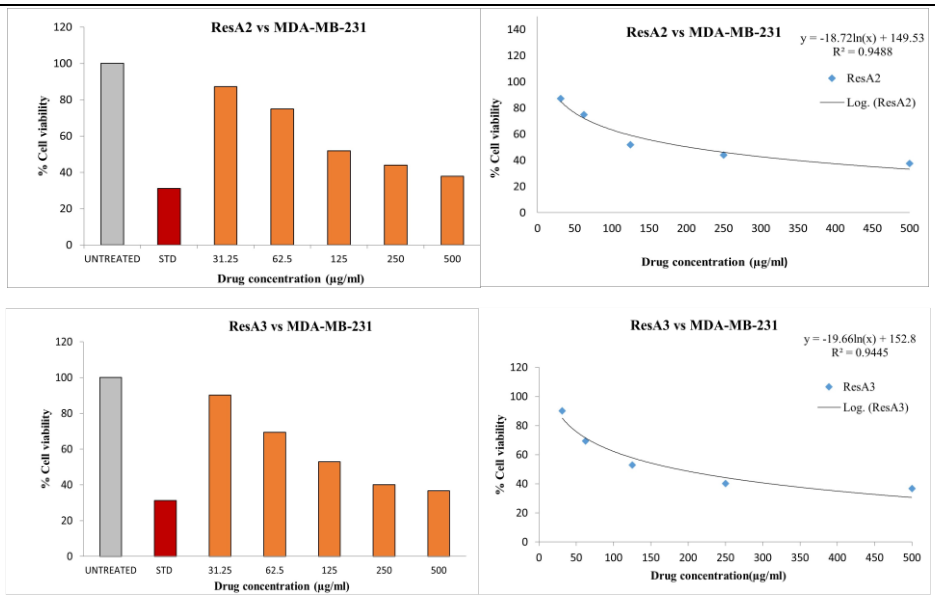

Figure 11.

Cell viability *vs*. drug concentration graphs in a dose-dependent manner and IC50 graphs of ResA2 (IC50 = 203.72 µg/mL) and ResA3 (186.58 µg/mL); Tamoxifen as a standard drug against MDA-MB-231 cells

Conclusions

The current study used pharmacophore-based design and synthesis of hybrid compounds using resveratrol as a scaffold to obtain a potential anti-breast cancer molecule against MCF-7 cells. For the first time, by using resveratrol as a scaffold (a phytochemical extracted, isolated and purified from fresh green grapes) three new hybrid molecules comprising resveratrol and aromatic hetero entities (ResA1, ResA2 and ResA3) were synthesized and their structures were elucidated by ^{1}H-NMR, ^{13}C-NMR, FTIR and LC-MS.

Among all designed resveratrol analogues, three molecules (ResA1, ResA2 and ResA3) obtained the highest docking scores, even higher than those of resveratrol and tamoxifen, and were thus identified as hit molecules and further taken for synthesis. ADME studies suggest that all three synthesized drug molecules have the proper volume of distribution values (VD) and can act on the Central Nervous System (CNS). DPPH free radical scavenging activities showed that ResA2 and ResA3 possess excellent antioxidant potential with IC50 values of 39.54 µg/mL, 26.82 µg/mL respectively. ZOI obtained from the disc diffusion method for the antimicrobial study revealed that ResA2 and ResA3 can effectively kill pathogens but do not affect non-pathogens. *In vitro* antiproliferative activity was carried out using the MTT assay against a panel of ER-positive and ER-negative human breast cancer cell lines. Persuasive IC50 values of ResA3 (327.70 µg/mL for MCF-7; 186.58 µg/mL for MDA-MB-231) and ResA2 (390.16 µg/mL for MCF-7; 203.72 µg/mL for MDA-MB-231) suggest their convincing anti-proliferative effect against human breast cancer cell lines. Even at 500 µg/mL, all three novel resveratrol analogues demonstrated greater than 70% cell viability against MCF-10A cells. Hence, the present study opens a new avenue to develop novel and superior anticancer drug molecules by performing different structural modifications in the base structure of resveratrol, which might lead to the discovery of more potent anti-breast cancer molecules. Moreover, anti-cancer mechanistic detail studies hold promises for further investigation.

Acknowledgement

This research was partially funded by grants from the Karnataka Science and Technology Academy (KSTA), the Government of Karnataka, India (Grant no. Karnataka Vijnana Mattu Tantrajnana Academy/ program/31/2021-2022), and M.S. Ramaiah University of Applied Sciences, Bangalore, India.

Conflict of interest

The authors declare no conflict of interest.

References

1. Abdollahi S, Salehi-Abargouei A, Toupchian O, Sheikhha MH, Fallahzadeh H, Rahmanian M, Tabatabaie M, Mozaffari-Khosravi H, The Effect of Resveratrol Supplementation on Cardio-Metabolic Risk Factors in Patients with Type 2 Diabetes: A Randomized, Double-Blind Controlled Trial. *Phytother Res.*, 2019; 33(12) :3153-3162.
2. Aggarwal BB, Bhardwaj A, Aggarwal RS, Seeram NP, Shishodia S, Takada Y, Role of resveratrol in prevention and therapy of cancer: Preclinical and clinical studies. *Anticancer Res*., 2004; 24: 2783-2840.
3. Aldawsari FS, Velázquez-Martínez CA, 3,4',5-trans-Trimethoxystilbene; a natural analogue of resveratrol with enhanced anticancer potency. *Invest New Drugs*, 2015; 33: 775-786.

4. Alley MC, Scudiere DA, Monks A, Czerwinski M, Shoemaker R, Boyd MR, Validation of an automated microculture tetrazolium assay (MTA) to assess growth and drug sensitivity of human tumour cell lines. *Proc Am Assoc Cancer Res.*, 1986; 27: 389.
5. Athar M, Back JH, Kopelovich L, Bickers DR, Kim AL, Multiple molecular targets of resveratrol: anti-carcinogenic mechanisms. *Arch Biochem Biophys.*, 2009; 486(2): 95-102.
6. Balouiri M, Sadiki M, Ibnsouda SK, Methods for *in vitro* evaluating antimicrobial activity: A review. *J Pharm Anal.*, 2016; 6(2): 71-79.
7. Banerjee S, Tian T, Wei Z, Shih N, Feldman M, Peck K, DeMichele A, Robertson E, Distinct microbial signatures associated with different breast cancer types. *Front Microbiol.*, 2018; 9: 951.
8. Bayat MR, Homayouni TS, Baluch N, Morgatskaya E, Kumar S, Das B, Yeger H, Combination therapy in combating cancer. *Oncotarget.*, 2017; 8(23): 38022-38043.
9. Berman HM, Henrick K, Nakamura H, Announcing the worldwide Protein Data Bank. *Nat Struct Biol.*, 2003; 10(12): 980.
10. Bilal I, Chowdhury A, Davidson J, Whitehead S, Phytoestrogens and prevention of breast cancer: The contentious debate. *World J Clin Oncol.*, 2014; 5(4): 705-712.
11. Bishayee A, Politis T, Darvesh AS, Resveratrol in the chemoprevention and treatment of hepatocellular carcinoma. *Cancer Treat Rev.*, 2010; 36: 43-53.
12. Cai YJ, Wei QY, Fang JG, Yang L, Liu ZL, Wyche JH, Han Z, The 3,4-dihydroxyl groups are important for trans-resveratrol analogues to exhibit enhanced antioxidant and apoptotic activities. *Anticancer Res.*, 2004; 24: 999-1002.
13. Chai EZP, Siveen KS, Shanmugam MK, Arfuso F, Sethi G, Analysis of the intricate relationship between chronic inflammation and cancer. *Biochem J.*, 2015; 468(1): 1-15.
14. Chen FP, Chien MH, Phytoestrogens induce differential effects on both normal and malignant human breast cells *in vitro*. *Climacteric.*, 2014; 17(6): 682-691.
15. Coimbra M, Isacchi B, van Bloois L, Torano JS, Ket A, Wu X, Broere F, Metselaar JM, Rijcken CJ, Storm G, Bilia R, Schiffelers RM, Improving solubility and chemical stability of natural compounds for medicinal use by incorporation into liposomes. *Int J Pharm.*, 2011; 416: 433-442.
16. Drăgan F, Moisa CF, Teodorescu A, Burlou-Nagy C, Fodor KI, Marcu F, Popa DE, Teaha DIM, Evaluating *in vitro* antibacterial and antioxidant properties of *Origanum vulgare* volatile oil. *Farmacia*, 2022; 70(6): 1114-1122.
17. Fasching PA, Heusinger K, Haeberle L, Niklos M, Hein A, Bayer CM, Rauh C, Schulz-Wendtland R, Bani MR, Schrauder M, Kahmann L, Lux MP, Strehl JD, Hartmann A, Dimmler A, Beckmann MW, Wachter DL, Ki67, chemotherapy response, and prognosis in breast cancer patients receiving neoadjuvant treatment. *BMC Cancer*, 2011; 11: 486.
18. Holder IA, Boyce ST, Agar well diffusion assay testing of bacterial susceptibility to various antimicrobials in concentrations non-toxic for human cells in culture. *Burns*, 1994; 20(5): 426-29.
19. Hsieh YS, Yang SF, Sethi G, Hu DN, Natural bioactive in cancer treatment and prevention. *Bio Med Res Int.*, 2015; 2015: 182835.
20. Jeandet P, Douillet-Breuil AC, Bessis R, Debord S, Sbaghi M, Adrian M, Phytoalexins from the *Vitaceae*: Biosynthesis, phytoalexin gene expression in transgenic plants, antifungal activity, and metabolism. *J Agric Food Chem.*, 2002; 50: 2731-2741.
21. Kapetanovic IM, Muzzio M, Huang Z, Thompson TN, McCormick DL, Pharmacokinetics, oral bioavailability, and metabolic profile of resveratrol and its dimethylether analogue, pterostilbene, in rats. *Cancer Chemother Pharmacol.*, 2011; 68: 593-601.
22. Kedare SB, Singh RP, Genesis and development of DPPH method of antioxidant assay. *J Food Sci Technol.*, 2011; 48(4): 412-422.
23. Kimberley RC, Computer Review of ChemDraw Ultra 12.0. *J Am Chem Soc.*, 2011; 133(21): 8388.
24. Lachenmeier DW, Godelmann R, Witt B, Riedel K, Rehm J, Can resveratrol in wine protect against the carcinogenicity of ethanol? A probabilistic dose-response assessment. *Int J Cancer*, 2014; 134: 144-153.
25. Mabona U, Viljoen A, Shikanga E, Marston A, Van Vuuren S, Antimicrobial activity of southern African medicinal plants with dermatological relevance: From an ethnopharmacological screening approach, to combination studies and the isolation of a bioactive compound. *J Ethnopharmacol.*, 2013; 148(1):45-55.
26. Magaldi S, Mata-Essayag S, Hartung de Capriles C, Perez C, Colella MT, Olaizola C, Ontiveros Y, Well diffusion for antifungal susceptibility testing. *Int J Infect Dis.*, 2004; 8(1): 39-45.
27. Melissa FA, Katja LL, Sarah NB, Florian K, Sebastian S, Haupt VJ, Schroeder M, PLIP 2021: expanding the scope of the protein-ligand interaction profiler to DNA and RNA. *Nucleic Acids Res.*, 2021; 49: 530-534.
28. Molino S, Dossena M, Buonocore D, Ferrari F, Venturini L, Ricevuti G, Verri M, Polyphenols in dementia: From molecular basis to clinical trials. *Life Sci.*, 2016; 161: 69-77.
29. Mosmann T, Rapid colorimetric assay for cellular growth and survival: application to proliferation and cytotoxicity assays. *J Immunol Methods*, 1983; 65(1-2): 55-63.
30. Mrkus L, Batinic J, Bjelis N, Jakas A, Synthesis and biological evaluation of quercetin and resveratrol peptidyl derivatives as potential anticancer and antioxidant agents. *Amino Acids*, 2019; 51(2): 319-29.
31. Nawaz W, Zhou Z, Deng S, Ma X, Ma X, Li C, Shu X, Therapeutic versatility of resveratrol derivatives. *Nutrients*, 2017; 9(11): 1188.
32. Nazzaro F, Fratianni F, De Martino L, Coppola R, De Feo V, Effect of Essential Oils on Pathogenic Bacteria. *Pharmaceuticals*, 2013; 6(12): 1451-1474.
33. Neves AR, Lúcio M, Martins S, Lima JL, Reis S, Novel resveratrol nano delivery systems based on lipid nanoparticles to enhance its oral bioavailability. *Int J Nanomed.*, 2013; 8: 177-187.
34. Newman DJ, Cragg GM, Natural Products as Sources of New Drugs from 1981 to 2014. *J Nat Prod.*, 2016; 79: 629-661.

35. Oh WY, Shahidi F, Antioxidant activity of resveratrol ester derivatives in food and biological model systems. *Food Chem.*, 2018; 261: 267-273.
36. Ombra MN, Di Santi A, Abbondanza C, Migliaccio A, Avvedimento EV, Perillo B, Retinoic acid impairs estrogen signalling in breast cancer cells by interfering with activation of LSD1 *via* PKA. *Biochim Biophys Acta.*, 2013; 1829: 480-486.
37. Palfi MC, Racea RC, Drăghici G, Seclaman EP, Munteanu M, Mușat O, Polyphenols content and in vitro antitumour activity of hydroalcoholic extract of *Viscum album* in two pigmented and unpigmented skin cancer cell lines. *Farmacia*, 2022; 70(5): 807-815.
38. Patani N, Martin L, Dowsett M, Biomarkers for the clinical management of breast cancer: International perspective. *Int J Cancer*, 2013; 133(1): 1-13.
39. Qin X, Hao X, Han H, Zhu S, Yang Y, Wu B, Hussain S, Parveen S, Jing C, Ma B, Zhu C, Design and Synthesis of Potent and Multifunctional Aldose Reductase Inhibitors Based on Quinoxalinones. *J Med Chem.*, 2015; 58(3): 1254-1267.
40. Remsberg CM, Martinez SE, Akinwumi BC, Anderson HD, Takemoto JK, Sayre CL, Preclinical pharmacokinetics and pharmacodynamics and content analysis of gnetol in foodstuffs. *Phytother Res.*, 2015; 29: 1168-1179.
41. Rivière C, Pawlus AD, Mérillon JM, Natural stilbenoids: Distribution in the plant kingdom and chemotaxonomic interest in *Vitaceae*. *Nat Prod Rep*, 2012; 29(11): 1317-1333.
42. Runyoro DK, Matee MI, Ngassapa OD, et al. Screening of Tanzanian medicinal plants for anti-Candida activity. *BMC Complement Alter Med.*, 2006; 6: 11.
43. Schmidt B, Ferreira C, Alves Passos CL, Silva JL, Fialho E, Resveratrol, curcumin and piperine alter human glyoxalase 1 in MCF-7 breast cancer cells. *Int J Mol Sci.*, 2020; 21: 5244.
44. Shanmugam MK, Rane G, Kanchi MM, Arfuso F, Chinnathambi A, Zayed ME, Alharbi SA, Tan BK, Kumar AP, Sethi G, The multifaceted role of curcumin in cancer prevention and treatment. *Molecules*, 2015; 20: 2728-2769.
45. Shi XP, Miao S, Wu Y, Zhang W, Zhang XF, Ma HZ, Xin HL, Feng J, Wen AD, Li Y, Resveratrol Sensitizes Tamoxifen in Antiestrogen-Resistant Breast Cancer Cells with Epithelial-Mesenchymal Transition Features. *Int J Mol Sci.*, 2013; 14: 15655-15668.
46. Shrivastav A, Bruce M, Jaksic D, Bader T, Seekallu S, Penner C, Nugent Z, Watson P, Murphy L, The mechanistic target for rapamycin pathway is related to the phosphorylation score for estrogen receptor-α in human breast tumors *in vivo*. *Breast Cancer Res.*, 2014; 16: 49.
47. Silva F, Figueiras A, Gallardo E, Nerín C, Domingues FC, Strategies to improve the solubility and stability of stilbene antioxidants: A comparative study between cyclodextrins and bile acids. *Food Chem.*, 2014; 145: 115-1125.
48. Tang YW, Shi CJ, Yang HL, Cai P, Liu QH, Yang XL, Kong LY, Wang XB, Synthesis and evaluation of isoprenylation-resveratrol dimer derivatives against Alzheimer's disease. *Eur J Med Chem.*, 2019; 163: 307-319.
49. The Open Babel Package, vers. 2.3.1 http://openbabel.org.
50. Turcov D, Barna S, Profire L, Iacob AT, Lisă G, Puițel AC, Zbranca A, Suteu D, Physico-chemical characterization of the antioxidant mixture resveratrol-ferulic acid for applications in dermato-cosmetic products. *Farmacia*, 2022; 70(3): 410-416.
51. Vestergaard M, Ingmer H, Antibacterial and antifungal properties of resveratrol. *Int J Antimicrob Agents*, 2019; 53(6): 716-723.
52. Von Gadow A, Joubert E, Hansmann CF, Comparison of the antioxidant activity of aspalathin with that of other plant phenols of rooibos tea (*Aspalathus linearis*), alpha-tocopherol, BHT, and BHA. *J Agric Food Chem.*, 1997; 45: 632-638.
53. Wenzel E, Somoza V, Metabolism and bioavailability of trans-resveratrol. *Mol Nutr Food Res.*, 2005; 49: 472-481.
54. Wicklow B, Wittmeier K, T' Jong GW, McGavock J, Robert M, Duhamel T, Dolinsky VW, Proposed trial: safety and efficacy of resveratrol for the treatment of non-alcoholic fatty liver disease (NAFLD) and associated insulin resistance in adolescents who are overweight or obese adolescents - rationale and protocol. *Biochem Cell Biol.*, 2015; 93(5): 522-530.
55. Wu H, Chen L, Zhu F, Han X, Sun L, Chen K, The Cytotoxicity Effect of Resveratrol: Cell Cycle Arrest and Induced Apoptosis of Breast Cancer 4T1 Cells. *Toxins*, 2019; 11(12): 731.
56. Xiong G, Wu Z, Yi J, Fu L, Yang Z, Hsieh C, Yin M, Zeng X, Wu C, Lu A, Chen X, Hou T, Cao D, ADMETlab 2.0: an integrated online platform for accurate and comprehensive predictions of ADMET properties. *Nucleic Acids Res.*, 2021; 49(1): 5-14.
57. Yang SF, Weng CJ, Sethi G, Hu DN, Natural bioactives and phytochemicals serve in cancer treatment and prevention. *Evid Based Complement Alternat Med.*, 2013; 2013: 698190.
58. Yen GC, Duh PD, Scavenging Effect of Methanolic Extracts of Peanut Hulls on Free-Radical and Active-Oxygen Species. *J Agric Food Chem.*, 1994; 42: 629-632.
59. Zhang Y, Shang Z, Gao C, Du M, Xu S, Song H, Liu T, Nanoemulsion for solubilization, stabilization, and invitro release of pterostilbene for oral delivery. *AAPS Pharm Sci Tech.*, 2014; 15(4): 1000-1008.
60. Zhao E, Mu Q, Phytoestrogen biological actions on Mammalian reproductive system and cancer growth. *Sci Pharm.*, 2011; 79(1): 1-20.
61. https://cytecare.com.
62. https://www.who.int.